The current issue and full text archive of this journal is available at
www.emeraldinsight.com/0961-5539.htm

Fin angle effect on turbulent heat transfer in parallel-plate channel with flow-inclining fins

Z.X. Yuan, L.H. Zhao and B.D. Zhang
College of Environmental and Energy Engineering, Beijing University of Technology, Beijing, People's Republic of China

Received April 2005
Revised March 2006
Accepted April 2006

Abstract

Purpose – This paper aims to develop enhanced surfaces that possess improved heat transfer rate with moderate flow pressure-drop.

Design/methodology/approach – The characteristics of the heat transfer and flow resistance in a parallel-plate channel with flow-inclining fins have been numerically and experimentally studied. In the turbulent flow range, the effect of the fin angle from 0 to 23.2° in addition to three channel heights, has been investigated.

Findings – The friction factor and the Nusselt number of the experimented 3D finned ducts are both lower than those of the numerical 2D channel at the same Reynolds number. The assessment under the constraint of the same pump power consumption shows that the enhancement ratio, Nu_m/Nu_0, is in between 1.6 ~ 3.3. Showing different priority, the fin of $\beta = 23.2°$ is the most profitable for the 2D channel, while the case of $\beta = 16.0°$ is superior to the other fin angles for thicker 3D ducts.

Research limitations/implications – For wide flat channels the 3D fins rather than the 2D fins are profitable. The deployment of the 3D fin, which is unchangeable in the current study, should be further optimized. The fin dimension and configuration in other duct forms are also challenging subjects.

Practical implications – The results can be referenced by those who engage in design of plate-fin heat exchangers. Attention should be paid to the optimum fin angle for different aspect ratios of the duct.

Originality/value – The study provides a practical fulfillment of the effective enhancement of the convective heat transfer with properly designed inserts that the field synergy principle predicted.

Keywords Turbulence, Heat transfer, Channel flow

Paper type Research paper

Nomenclature

A = area, m^2
C_p = specific heat, J/kg K
D_e = equivalent diameter of the duct, m
f = friction factor, dimensionless
h = heat transfer coefficient, W/m^2K
h_1 = back height of the fin, mm
H = half duct height, mm
Int_0 = integral of field synergy, equation (10)m^2 K/s
k = thermal conductivity, W/m K
K = turbulent kinetic energy, J/kg
Nu = Nusselt number, dimensionless
p = pressure, Pascal
q = heat flux, W/m^2
Re = Reynolds number, dimensionless
T = temperature, K
∇T = temperature gradient, K/m
$\vec{U}$ = velocity vector, m/s

This work is sponsored by the Beijing Natural Science Foundation (No. 3052002) and the Beijing Municipal Commission of Education (No. KM200410005020).

International Journal of Numerical Methods for Heat & Fluid Flow
Vol. 17 No. 1, 2007
pp. 5-19

0961-5539
DOI 10.1108/09615530710716054

u, v = velocity component, m/s
x, y = Cartesian coordinate, mm
y_p^+ = dimensionless distance of the first node to the wall

Greek symbols
β = inclining angle of the fin, °
δ_t = thermal boundary layer thickness, m
ε = turbulent dissipation rate, W/kg
μ = dynamic viscosity, Pa s
ν = kinematic viscosity, m^2/s
θ = included angle between $\vec{U}$ and ∇T, °
ρ = fluid density, kg/m^3

Subscripts
0 = smooth duct
m = mean
p = node closest to the wall
w = wall
t = turbulent

1. Introduction

The main purpose for the study of the convective heat transfer enhancement is usually to find configurations with high heat transfer rate and low friction factor. Many researchers have made efforts till today to reach this goal. One of the approaches is the adoption of wavy channel (Xin and Tao, 1988) or non-uniform cross section (Meng *et al.*, 2005). The wavy channel or the change of the cross section causes the fluid flow to wash against the solid wall effectively, and then promote the heat transfer on the surface. Internal insert is another way to enhance the heat transfer in tubes. Some researchers, including Sparrow and Tao (1984), Zeitoun and Hegazy (2004), Yuan *et al.* (1998) and Yuan (2000), studied the enhanced duct with longitudinal fins or transverse disturbances. These internal inserts really enhance the heat transfer effectively, but usually with strong pressure-drop penalty. Imposing a special force field onto the flow is also an effective way to the enhancement. Yang *et al.* (2004) and Molki and Bhamidipati (2004) experimentally studied the magnetic field and corona wind effect on the heat transfer, respectively. Yang *et al.* (2004) found that the quadruple magnetic field acting on the airflow in a duct could drive its span-wise flow and enhance the heat transfer. Molki and Bhamidipati (2004) reported that the corona wind formed in an electric field up to 10.5 kV increased the local heat transfer coefficient in the developing region by 14-23 percent.

Any enhancement effect should be evaluated with the consideration of both the heat transfer increment and the pressure-drop penalty. The ratio of the heat transfer coefficient and the friction factor for a configuration can be called as its input-output ratio, which is an index to the thermal performance of the configuration. For a given configuration, is there a maximum of the input-output ratio under a physical condition? How to reach this maximum? These are interesting and essential questions for the discipline of heat transfer. A novel theory with respect to the mechanism of convective heat transfer, which was established by Guo and his co-workers (Guo *et al.*, 1998; Guo, 2001; Wang *et al.*, 1998), may be helpful to answer these questions. This theory is called the Field Synergy Principle. The aforementioned enhancement with different approaches can also be properly explained by this theory, in that all of them have increased the velocity component normal to the wall as well as the field synergy degree. Through analyzing the heat transfer in boundary layer, Guo *et al.* (1998) found that there exists a relationship between the wall heat flux q_w and the product of the velocity vector and the temperature gradient as following:

$$\rho C_p \int_0^{\delta_t} (\vec{U} \cdot \nabla T) \mathrm{d}y = q_w \tag{1}$$

This relation tells us that the convective heat flux on the solid wall depends not only on the fluid velocity itself, but also on the included angle between the velocity and the temperature gradient. By the vector operation principal, we have $\vec{U} \cdot \nabla T = |U||\nabla T| \cos \theta$. Decreasing the included angle is beneficial to the heat transfer. Guo (2001) proposed three ways to reach this purpose: use of gradually constricting duct; reasonable variation of the thermal boundary condition; and use of specially designed inserts. The optimization of thermal boundary condition for the enhancement was discussed in a recent paper by Yuan *et al.* (2004). It revealed that the exponentially rising surface heat flux do improve the synergy degree and then enhance the heat transfer. Tao *et al.* (2002a, b) extended this theory from parabolic flow to elliptic flow and conducted a unified analysis for the single-phase convection. Based on the field synergy principle, Cheng *et al.* (2004) have designed a slotted fin surface that shows advancement in view of the input-output ratio.

In the current study, an enhanced surface developed based on the field synergy principle is numerically and experimentally investigated about its turbulent heat transfer and resistance characteristics. The numerical study is to the 2D problem in the periodically fully developed regime as shown in Figure 1. Figure 2 is the representative photo of the test surface, and Figure 3 is the deployment of the fin and the fin dimensions. The fin on the test surface is intermittent transversely rather than a whole plank in the 2D numerical simulation. The study is focused on the effect of the fin angle, β and the duct height, $2H$.

2. Experimental and numerical method

2.1 Experimental method

The experiment has been conducted in a wind tunnel. As shown in Figure 3, the test duct is 320 mm long and 100 mm wide. The flow-inclining fin is arranged in three arrays with 10 mm space between. The duct has three heights of 20, 30, and 40 mm. Taking into account the substrate thickness, the net half height of the duct is 7, 12, and 17 mm. The front fin height keeps the constant of 6 mm. The fin angle β is regulated with the change of the downstream height of the fin h_1, which takes 3, 4, 5 and 6 mm, corresponding to $\beta = 23.2$, 16.0, 8.1, and 0°. The fin as well as the substrate are made of copper and braze welded together. The upper and lower finned wall is electrically heated to form a uniformity heat flux condition. The sidewalls are Lucite plate of 4 mm thick and kept adiabatic in the experiment. The substrate plate and the sidewall are

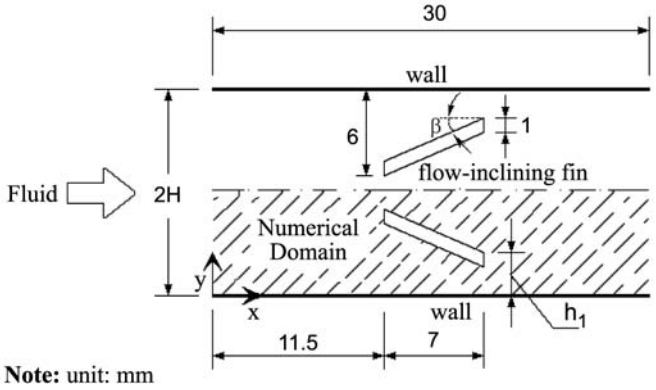

Figure 1.
Schematic of a cycle structure and the numerical domain in the 2D channel

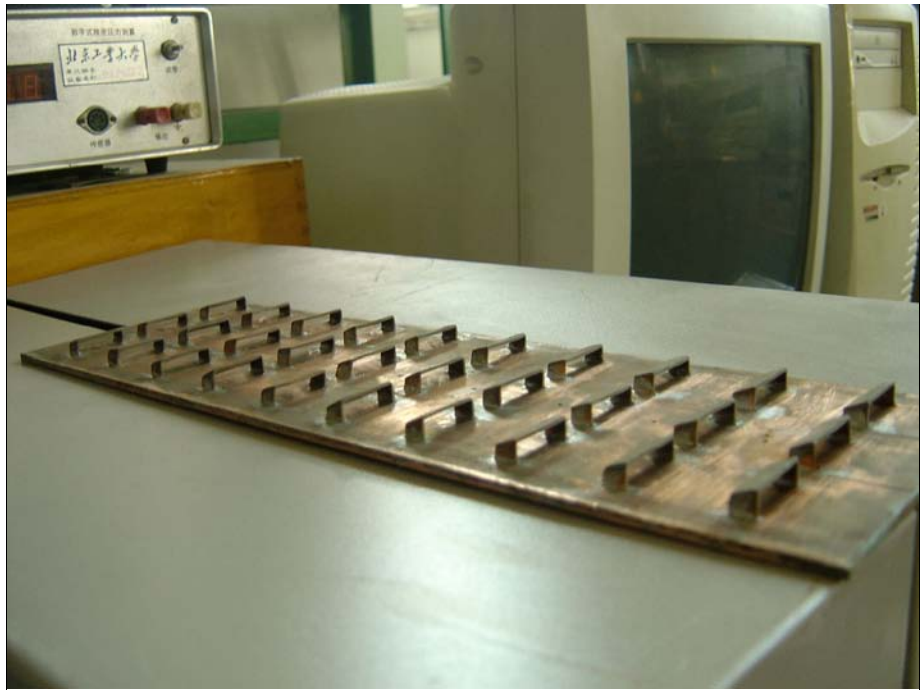

Figure 2.
The experimental enhanced duct wall with 3D flow-inclining fins

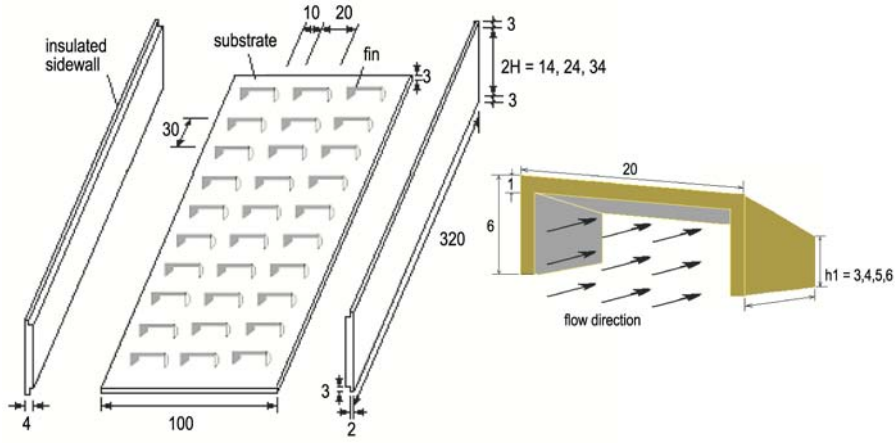

(a) Arrangement of the fin (b) The fin dimensions

Note: unit: mm

Figure 3.
Arrangement of the fin on the tested duct wall

connected in epoxy so that the whole duct is airtight. Outside the heating belt of nickel-chromium alloy, there is a 20 mm thick insulation of asbestos material to reduce the heat loss.

Tap holes of 1 mm in diameter are drilled on the top wall to measure the longitudinal variation of the pressure. There is a tap hole for each cycle. An inclining tube manometer is responsible for the pressure measuring. Nineteen pairs of copper-constantan thermocouples are embedded onto the bottom wall along the centerline, and they are connected to the data acquisition system to record the temperature variation on the inner surface. There are also four thermocouples evenly distributed across the section of the inlet and outlet of the test duct so that the changes of the air can be determined. A Pitot tube is employed to measure the flow velocity.

With the basic estimations of the uncertainty of the pertinent parameters, the uncertainty of the derived variables has been analyzed according to the method proposed by Kline and McClintock (1953). The result gives the heat flux the uncertainty of 5.0 percent, the heat transfer coefficient of 6.2 percent, the Nusselt number of 7.3 percent, the Reynolds number of 4.5 percent, and the friction factor of 8.6 percent.

2.2 Numerical method

For channels with periodical disturbances, the fluid flow can reach periodically fully developed regime after a few cycles from the entrance, as reported by Sparrow and Tao (1984), and Liu *et al.* (1993). In this regime, the pressure-drop and the mean heat transfer rate for each cycle is the same. The flow resistance and the thermal performance of a periodically disturbed configuration are usually represented by its characteristics in the fully developed regime. Therefore, in the numerical part of the current study the attention will be focused on a cycle as shown in Figure 1. In consideration of the symmetry, the simulated domain takes only a half of the cycle. The simulated working fluid is water.

The $K - \varepsilon$ model, together with the wall function approach, has been adopted to solve this turbulent problem. In the $K - \varepsilon$ model, the keystone is the way to determine the turbulent viscosity, μ_t through the turbulent kinetic energy, K and the dissipation rate, ε. Their relation satisfies the Prandtl-Kolmogrov formula

$$\mu_t = c_\mu \rho K^2/\varepsilon \tag{2}$$

c_μ is one of the turbulent constants, and $c_\mu = 0.09$. As the $K - \varepsilon$ model is only suitable for the high Reynolds number flow, the parameters in the vicinity region of the solid wall, where the molecular viscosity functions mainly, need to be handled specifically. A common method for handling the wall-closed parameter is the Wall Function Approach (Launder and Spalding, 1974). This method requires that all node points in the domain must fall in the fully turbulent region. Concretely, the propriety of the location of the first node p is evaluated by its dimensionless distance from the solid wall as following:

$$y_p^+ = \frac{y_p c_\mu^{1/4} K_p^{1/2}}{\nu} \tag{3}$$

where y_p denotes the normal distance of node p to the wall. All y_p^+should satisfy $11.5 \leq y_p^+ \leq 400\, K_p$ is obtained through solving the K equation with the boundary condition of $(\partial K/\partial y)_w = 0$, and ε_p is determined from the function:

$$\varepsilon_p = \frac{c_\mu^{3/4} K_p^{3/2}}{0.42\nu} \tag{4}$$

Upon solution of the $K - \varepsilon$ equations, the turbulent diffusion parameter k_t and μ_t can be calculated by a series of function. Since, the governing equations are available in the open literature (Yuan, 2000), they are not presented here for briefness.

The principal wall is kept as an isothermal surface. The wall temperature is different from that of the inlet fluid. A given mass flow corresponds to a Reynolds number. The inlet and outlet of the domain are periodic boundary conditions. The numerical procedure basically follows what proposed by Patankar (1981). The software FLUENT, with SIMPLE algorithm, has been applied to the simulation. The Second Order Upwind was chosen as the discrete scheme for the momentum and energy equations, and the PRESTO! scheme was for the discretization of the pressure-revised equation. According with the velocity gradient, non-uniform grid systems, which change from fine to coarse gradually apart from the wall, have been adopted. The grid has been checked for its independence of the solution prior to the formal calculation. The typical grid system in the simulation was 150×64 for x and y direction, respectively. The criterion of convergence for the residual was 10^{-4} for the momentum equation and 10^{-7} for the energy equation.

2.3 Data reduction

The mean friction factor for a cycle is calculated by the Darcy definition:

$$f_m = \frac{-(\overline{dp}/dx) \cdot D_e}{1/2\rho\bar{u}^2} \tag{5}$$

where $\overline{dp}/dx$ is the average pressure gradient per cycle. D_e is the equivalent diameter of the channel. $\bar{u}$ is the average velocity at the inlet. The Reynolds number is defined as:

$$Re = \frac{\bar{u} \cdot D_e}{\nu} \tag{6}$$

The average heat transfer coefficient in a cycle is obtained from the numerical solution or from the experimental result. Based on the average heat transfer coefficient, the mean Nusselt number in a cycle is:

$$Nu_m = \frac{\overline{h}_w D_e}{k} \tag{7}$$

Here, k is the thermal conductivity of the fluid.

3. Numerical fields of flow and temperature

Figure 4 is the numerical vector plot of the flow field for the case of $\beta = 16.0°$ and $Re = 60{,}000$. Because of the fin blocking function, the fluid is basically divided into two parts. The proportion of the upper and the lower fluid is determined by the fin angle and the channel height. Larger angles may catch more fluids and incline them towards to the wall but result in higher flow resistance. For single-phase convective heat transfer, jet impingement possesses the highest heat transfer rate for a given flow velocity. If the flowing fluid in a duct could be turned towards to the principle wall

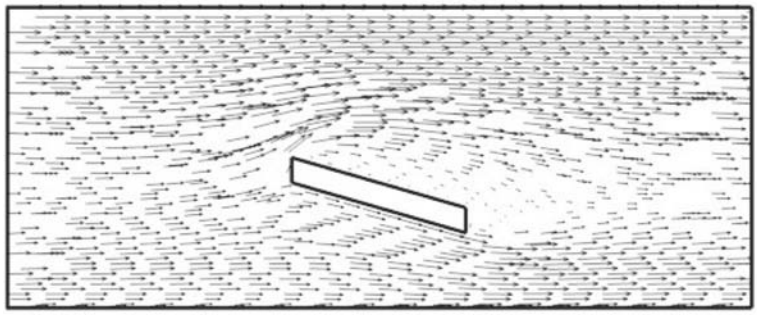

Notes: H = 12 mm, β = 16.0°, Re = 60,000

Figure 4.
Velocity field

everywhere, the heat transfer would be the optimal. Therefore, what we pay attention here is the lower stream near the bottom wall. It can be thought as a pseudo oblique jet impinging onto the wall. The oblique jet stream will definitely promote the heat transfer in comparison with the parallel flow. We hope the stream to impinge the wall perpendicularly, but it is very difficult to do so in a duct. If the fin angle is too large, it will cause the flow resistance increase sharply. And too large fin angle will cause the most fluid to flow away from the fin-and-wall tunnel. In order to balance the impinging portion and the flow resistance, optimizing the fin angle is necessary.

The isotherms of temperature corresponding to the velocity field in Figure 4 are shown in Figure 5. In the 2D channel, the inclining fin does not work as a path to transfer heat from the wall to the fluid, because there is no connection between the fin and the heated substrate. The fin shows adiabatic feature no matter what material it consists of. The function of the fin here is just to incline the fluid towards to the surface. In this point, the 2D channel is different from the experimental 3D finned duct, in which the fin plays both the role of flow incliner and heat distributor. In Figure 4, the isotherms near the bottom are much denser that those in the central part. This is a common feature for turbulent heat transfer. On the other hand, the isotherms near the bottom are not even. Those lines down stream of the fin show a cluster tendency. This suggests that the temperature gradient there has been promoted and the heat transfer has been improved locally.

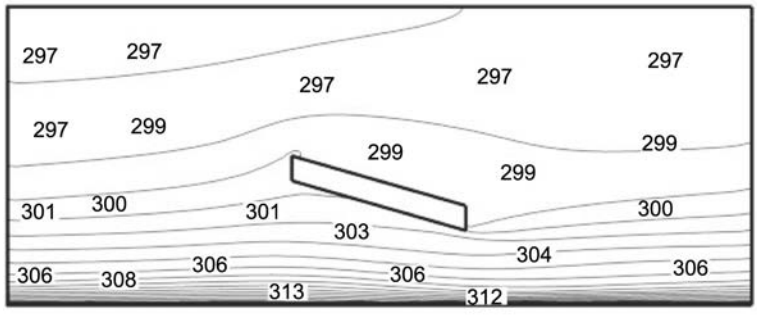

Notes: H = 12 mm, β = 16.0°, Re = 60,000

Figure 5.
Temperature field

4. Characteristics of resistance and heat transfer

4.1 The friction factor

From the view of practical application in engineering, it is feasible to evaluate the flow resistance with the mean friction factor in a cycle. The variation of the mean friction factor for the channel of $H = 12$ mm is shown in Figure 6. To facilitate the comparison, the friction factor for the smooth duct has also been plotted according to the Blasius equation:

$$f_0 = 0.3164\, Re^{-1/4} \tag{8}$$

The application of the flow-inclining fin causes the resistance to increase greatly. On the other hand, the friction factor of the 3D finned duct is obviously lower than that of the 2D channel. When the fin is intermittent instead of a whole one, a part of the fluid will tend to flow through the gap between the neighboring fins, because the fluid always takes the lower resistance path. Comparatively, in the 2D channel more fluid is forced to incline towards to the wall and then the flow resistance is increased as a result. As expected, the fin angle β is an important factor to impact the flow resistance. In the studied parameter range, the f_m increases with the β monotonically. The fin of $\beta = 23.2°$ produces a resistance 6-7 times of the fin of $\beta = 0°$ for the 2D channel. f_m tends to decrease with the Reynolds number increasing, but this tendency becomes less obvious for the higher fin angles.

4.2 The local Nusselt number

Figure 7 is a case of the local Nusselt number distribution in a cycle. Though the periodically fully developed flow is considered, the flow and the heat transfer are always developing within each cycle. As well known, the heat transfer coefficient in

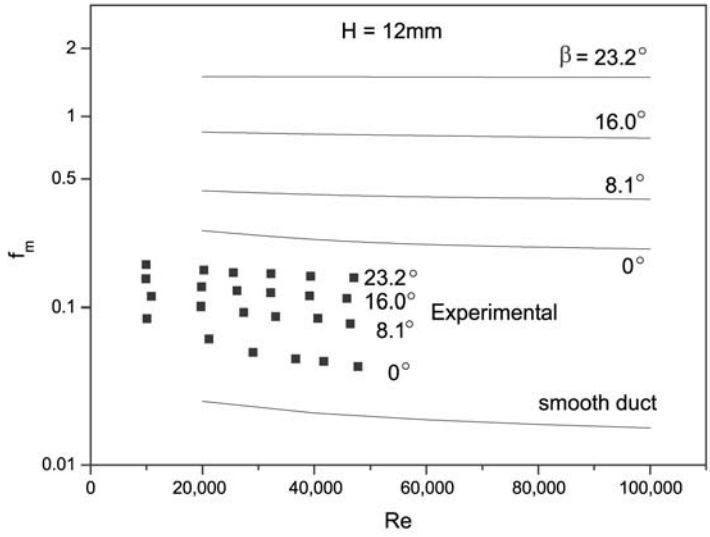

Notes: — Numerical result of the 2D channel; ■ Experimental result for the 3D finned channel. The data for the smooth duct is determined from the Blasius formula

Figure 6.
Mean friction factor in a cycle vs the Reynolds number at different fin angles

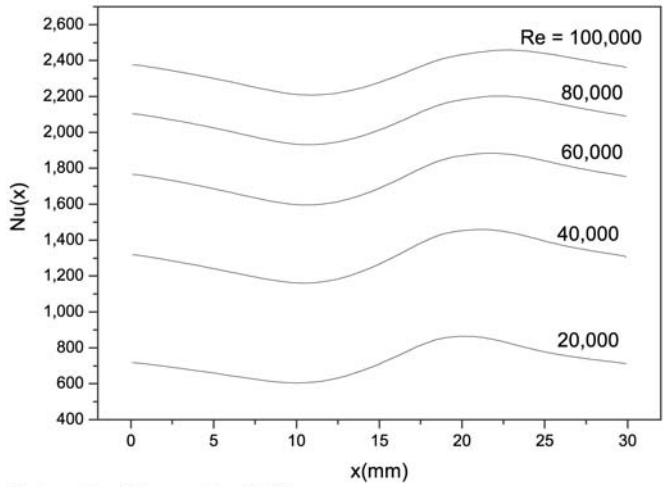

Notes: H = 12 mm, β = 16.0°

Figure 7.
Distribution of the local Nusselt number in a cycle

the developing region of a smooth duct declines along the flow direction due to the growth of the boundary layer. For the 2D channel shown in Figure 1, the variation of the local Nusselt number reflects the change of the boundary layer in the cycle. Outside the fin region, the Nusselt number decreases along the flow direction. Contrastively, the Nusselt number escalates within the fin area. From $x = 12$ mm, the Nusselt number climbs up and reaches its maximum at about $x = 22$ mm. For the internal convection enhancement what is paid attention is restraining the gradual degradation of the heat transfer rate. Here, we see that the inclining fin functions to increase the heat transfer locally, so the original purpose to keep the heat transfer in a relative high level is achieved.

The effect of the Reynolds number is intensive, too. The Nusselt number becomes higher as the Reynolds number increases, though the increment is smaller for higher Reynolds numbers. An interesting phenomenon is the shift of the *Nu* maximum. We can observe that the *Nu* maximum shifts downstream as the Reynolds number increases. All the maximums fall in between $x = 20$ and 23 mm corresponding to $Re = 2 \times 10^4 \sim 10^5$. High velocity produces large inertial force of the fluid, and then causes the thinnest point of the boundary layer to shift downstream when the fluid rushes out of the fin-and-wall tunnel.

4.3 The mean Nusselt number

The mean Nusselt number against to the Reynolds number in a cycle is shown in Figure 8. Since, the numerical simulation and the experiment have taken different working fluid, direct comparison of the Nusselt numbers is not suitable. Here, the $Nu_m/Pr^{1/3}$ is taken as the index to evaluate the averaged heat transfer characteristic. The numerical and the experimental results, together with the data of the smooth duct, are shown in the figure. The data of the smooth duct is determined by the Dittus-Boelter correlation

$$Nu_0 = 0.023\, Re^{0.8} Pr^{1/3} \tag{9}$$

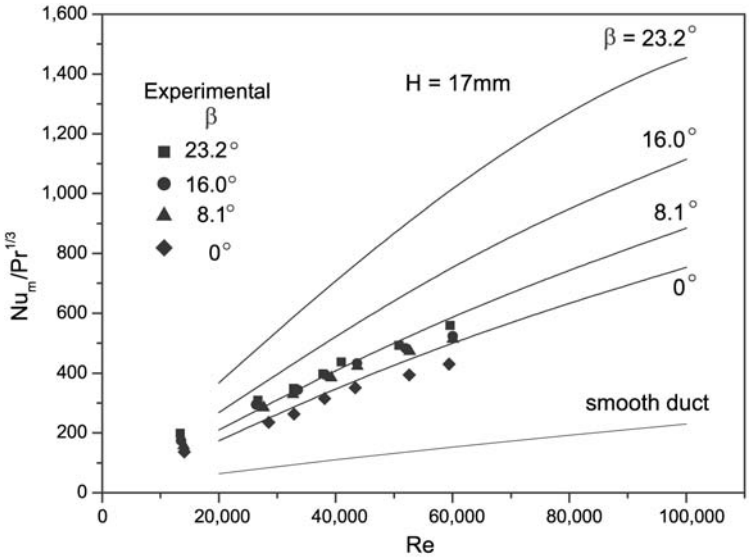

Figure 8.
Mean Nusselt number in a cycle vs the Reynolds number at different fin angles

Notes: — Numerical result of the 2D channel; ■ Experimental result for the 3D finned channel. The data for the smooth duct is determined from the Dittus-Boelter correlation

Though the $Nu_m/Pr^{1/3}$ of the 3D finned duct is still affected by the fin angle to some extent, the relationship between them is much less than that of the numerical results of the 2D channel. For the numerical results, the heat transfer rate increases markedly with the fin angle. The case of $\beta = 23.2°$ is the best and $\beta = 0°$ is of the least enhanced effect. Generally speaking, the cases of $\beta = 0$ and 8.1° of the experiment show comparable heat transfer rate to the numerical result. For the larger fin angles the $Nu_m/Pr^{1/3}$ have more discrepancy. However, the discrepancy tends to diminish as the Reynolds number decreases.

4.4 Assessment of the enhancement effect

As well known, the heat transfer is usually enhanced at the expense of increased flow resistance. The criterion to evaluate a configuration is upon how much pumping power is consumed to obtain the same heat transfer rate. For the current study, both the friction factor and the Nusselt number are increased due to application of the flow-inclining fin, as shown in Figures 6 and 8, respectively. To evaluate the enhancement effect reasonably, it is necessary to take into account the Nusselt number and the friction factor together. Here, the assessing method of the same pump power constraint is adopted. The detail of the method was discussed in a previous work of the present author (Yuan, 2000), and not repeated here. The ratio of the Nusselt number for the enhanced and the smooth duct, Nu_m/Nu_0, is still the assessing criterion. Prior to the calculation of the ratio, the Nu_0 needs to convert to its counterpart at the Reynolds number that the smooth duct would reach with the same power consumption as the enhanced channel. Since, the friction of the enhanced channel is always higher, the Reynolds number for the counterpart Nu_0 is always an increased value.

Therefore, the ratio of Nusselt number from this method is smaller than that obtained at the same Reynolds number condition. If the derived Nu_m/Nu_0 is above unity, the enhanced channel is profitable.

The assessed result is shown in Figure 9. For the three channel heights, all the Nu_m/Nu_0 are above unity for any fin angle at any Reynolds number. This suggests that the configuration of the flow-inclining fin can keep a relative high heat transfer rate in the range of the study. For the numerical results, the fin angle affects positively the enhancement ratio. The result of the fin of $\beta = 23.2°$ is superior to all the others. The influence of the Reynolds number to the Nu_m/Nu_0 is associated with the duct height. For the case of $H = 7$ mm, the Nu_m/Nu_0 declines monotonically with the Reynolds number. For $H = 12$ mm, it only declines monotonically after $Re = 50{,}000$. For $H = 17$ mm, the variation of $H = 7$ mm is non-monotonically all the way. The maximum of Nu_m/Nu_0 occurs in between $Re = 40{,}000 \sim 60{,}000$, while the Nu_m/Nu_0 does not change too much with Re. The channel of $H = 7$ mm produces the highest Nu_m/Nu_0 at the lower Reynolds numbers, but the ratio drops drastically as the Reynolds number increases.

Though the experimented Reynolds number range is not the same as the numerical, the basic tendency of the Nu_m/Nu_0 can be detected in the result. Generally, the assessed results for the experimental and the numerical are in the comparable scope. On the other hand, since the structure of the experimented duct does not follow the numerical channel exactly, the results show some discrepancy with each other. Different from the tendency of the numerical, all Nu_m/Nu_0 of the experiment decrease consistently with the Reynolds number. For the ducts of $H = 7$ and 12 mm, most Nu_m/Nu_0 of the experiment are lower than those of the numerical. However, the results for $H = 17$ mm are basically the opposite. This can be explained in the view of the fin efficiency. The 3D fin in the experimented duct is heat-conducting, while the 2D fin in the numerical is adiabatic. The thermal efficiency of the heat-conducting fin is related to the convective heat transfer on the fin surface. For the narrow duct of $H = 7$ mm, the fin intrudes into the central part of the duct, therefore, it is subjected to the fluid washing of high velocity and the efficiency is low. The function of the fin is mainly flow-inclining. The intermittent fin is of less inclining effect than the whole fin, and then the enhancement is inferior. In contrast, in the wider duct the fin is near the wall and washed not so strongly. Thus, the fin efficiency is relatively high and the fin heat transfer takes a non-ignorable part in addition to the flow-inclining function. Anyway, the effect of the flow-inclining fin to the heat transfer is obvious from the results.

The impact of the fin angle for the experimented duct is different from the numerical result. Only the duct of $H = 7$ mm remains the best effect of $\beta = 23.2°$. For the ducts of $H = 12$ and 17 mm, the fin of $\beta = 16.0°$ is the best. This is considered the comprehensive result when the friction and the heat transfer are combined together. As the fin angle increases towards 90° the flow resistance will increase sharply. The output and input ratio will declines over a critic fin angle. Therefore, it is reasonable that there exists a unique fin angle corresponding to the maximum enhancement effect. As to the influence of the duct height, the general tendency is that the fin angle seems to affect the Nu_m/Nu_0 less strongly for the narrow duct than for the wide. Nevertheless, most of the Nu_m/Nu_0 fall in between $2.0 \sim 2.7$ in the experimented Reynolds number range.

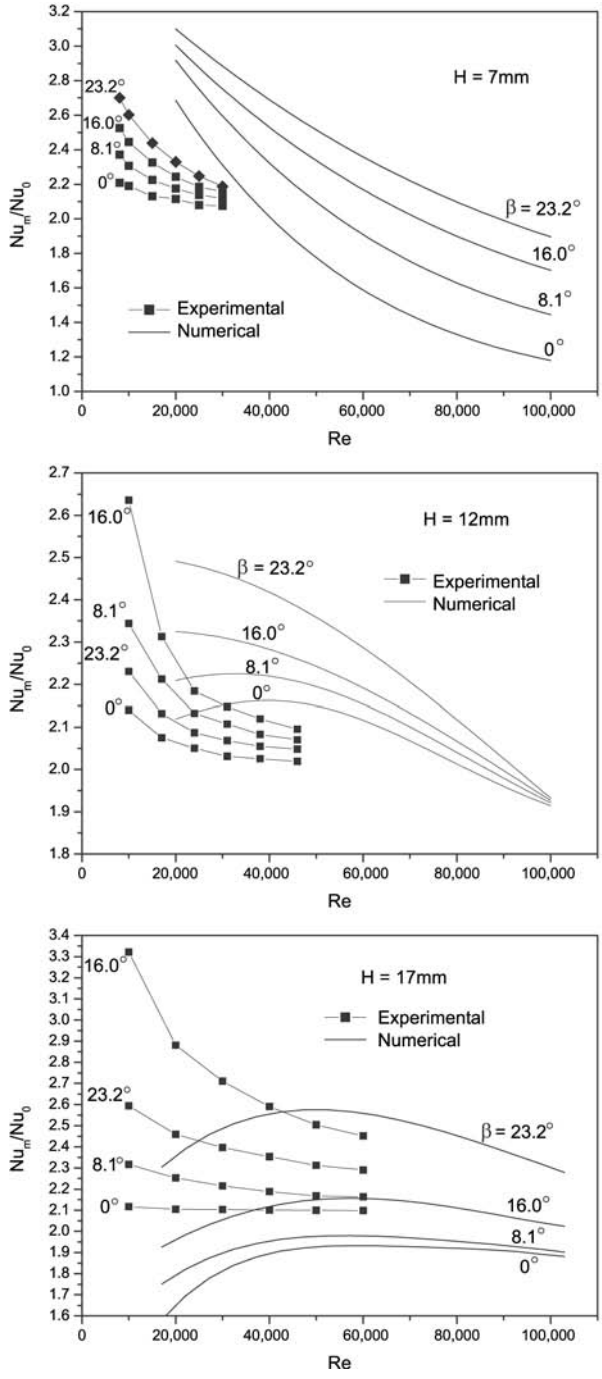

Figure 9.
Enhancement effect assessed under the same pump power consumption

5. Characteristics of the field synergy

As mentioned in the introduction, the configuration of the flow-inclining fin has been developed according to the field synergy principle. Therefore, checking the relationship of the Nusselt number and the field synergy is necessary. To facilitate the discussion, here we define an index Int_0 to represent the synergy degree:

$$\mathrm{Int}_0 = \iint_A (\vec{U} \cdot \nabla T) \mathrm{d}x\, \mathrm{d}y \tag{10}$$

where A denotes the numerical domain, and $\vec{U}$and$\nabla T$are all from the numerical result. The included angle θ between the velocity and the temperature gradient is determined by the vector operation $\vec{U} \cdot \nabla T = |U||\nabla T| \cos\theta$. The included angle is a crucial parameter to affect the synergy degree for a determined flow. Lower θ means higher Int_o and higher heat transfer on the surface. In the following the averaged θ over the domain, θ_m, is to be discussed.

The variation of θ_m is shown in Figure 10. From the view of the field synergy principle, enhancing the convective heat transfer is to find the effective way to minimize the included angle of the velocity and the ∇T, for the jet impingement, in which the θ_m is nearly to zero, is of the highest heat transfer rate for single-phase flow. The result in Figure 10 clearly shows that the inclining fin is really helpful to reduce the included angle. With the change of β from 0 to 23.2° the θ_m drops from 88.5° to less than 84°.Furthermore, the θ_m here are also consistent with the Nusselt number in Figure 7 with respect to the fin angle β. Higher β originates smaller θ_m, and cause the heat transfer to improve. A point worthy to note is the relation of the θ_m with the Reynolds number. Not as the effect of the fin angle β, the dependence of the θ_m on the Reynolds number is not appreciable. It suggests that the average included angle is insensitive to the Reynolds number in turbulent heat transfer.

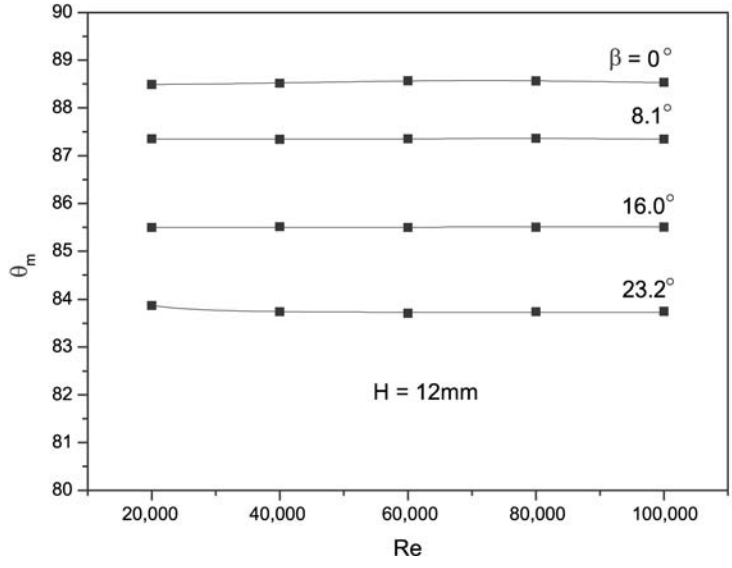

Figure 10.
Variation of the averaged θ with the Reynolds number

6. Conclusions

Following the principle of the field synergy for convective heat transfer, the thermal performance and flow resistance in the parallel-plate channel with flow-inclining fins have been numerically and experimentally studied in the turbulent flow range. Four fin angles of $\beta = 0$, 8.1, 16.0 and 23.2° in addition to three channel height, have been involved. The friction factor and the Nusselt number have been analyzed and evaluated:

- In a cycle, the local Nusselt number increases where the fin locates, and decreases apart from the fin region. The inclining fin acts like an escalator to recover the heat transfer during its degradation process.
- Larger fin angle always originates stronger heat transfer as well as flow resistance in the range of $\beta = 0 \sim 23.2°$. On the other hand, the friction factor and the Nusselt number of the experimented 3D finned ducts are both lower than those of the numerical 2D channel at the same Reynolds number.
- The assessment under the constraint of the same pump power consumption reveals that the enhancement ratio, Nu_m/Nu_0, is related to both the fin angle and the Reynolds number. For the 2D channel, the case of $\beta = 23.2°$ is of the best effect for all the three duct heights. For the 3D finned duct, the case of $\beta = 23.2$ or 16.0° is the best, depending upon the duct height.
- Small included angles between the fluid velocity and the temperature gradient correspond to the higher Nusselt number. Larger fin angle produces smaller included angle. The results illustrate the validity of the field synergy principle for the enhancement of convective heat transfer.

References

Cheng, Y.P., Qu, Z.G., Tao, W.Q. and He, Y.L. (2004), "Numerical design of efficient slotted fin surface based on the field synergy principle", *Numerical Heat Transfer Part A – Applications*, Vol. 45 No. 6, pp. 517-38.

Guo, Z.Y. (2001), "Mechanism and control of convective heat transfer – coordination of velocity and heat flow fields", *Chinese Science Bulletin*, Vol. 46 No. 7, pp. 596-9.

Guo, Z.Y., Li, D.Y. and Wang, B.X. (1998), "A novel concept for convective heat transfer enhancement", *Int. J. Heat Mass Transfer*, Vol. 41, pp. 2221-5.

Kline, S.J. and McClintock, F.A. (1953), "Describing uncertainties in single sample experiment", *Mechanical Engineering*, Vol. 75, pp. 3-9.

Launder, B.E. and Spalding, D.B. (1974), "The numerical computation of turbulent flows", *Computer Methods in Applied Mechanics and Engineering*, Vol. 3, pp. 269-89.

Liu, T.M., Huang, J.J. and Chen, S.H. (1993), "Simulation and measurement of enhanced turbulent heat transfer in a channel with periodic ribs on one principal wall", *Int. J. Heat Mass Transfer*, Vol. 36, pp. 507-17.

Meng, J.A., Liang, X.G., Chen, Z.J. and Li, Z.X. (2005), "Experimental study on convective heat transfer in alternating elliptical axis tubes", *Experimental Thermal and Fluid Science*, Vol. 29 No. 4, pp. 457-65.

Molki, M. and Bhamidipati, K.L. (2004), "Enhancement of convective heat transfer in the developing region of circular tubes using corona wind", *Int. J. Heat Mass Transfer*, Vol. 47 Nos 19/20, pp. 4301-14.

Patankar, S.V. (1981), "A calculation procedure for tow-dimensional elliptic situations", *Numerical Heat Transfer*, Vol. 4 No. 4, pp. 409-25.

Sparrow, E.M. and Tao, W.Q. (1984), "Symmetric vs asymmetric periodic disturbances at the walls of a heated flow passage", *Int. J. Heat Mass Transfer*, Vol. 27 No. 11, pp. 2133-44.

Tao, W.Q., Guo, Z.Y. and Wang, B.X. (2002a), "Field synergy principle for enhancing convective heat transfer – its extension and numerical verifications", *Int. J. Heat Mass Transfer*, Vol. 45, pp. 3849-56.

Tao, W.Q., He, Y.L., Wang, Q.W., Qu, Z.G. and Song, F.Q. (2002b), "A unified analysis on enhancing single phase convective heat transfer with field synergy principle", *Int. J. Heat Mass Transfer*, Vol. 45, pp. 4871-9.

Wang, S., Li, Z.X. and Guo, Z.Y. (1998), "Novel concept and device of heat transfer augmentation", *Proceedings of 11th IHTC*,Vol. 5, pp. 405-8.

Xin, R.C. and Tao, W.Q. (1988), "Numerical prediction of laminar flow and heat transfer in wavy channels of uniform cross-sectional area", *Numerical Heat Transfer*, Vol. 14, pp. 465-81.

Yang, L.J., Ren, J.X. and Song, Y.Z. (2004), "Field coordination of air convection heat transfer in rectangular channel with magnetic field", *J. Enhanced Heat Transfer*, Vol. 11 No. 4, pp. 331-40.

Yuan, Z.X. (2000), "Numerical study of periodically turbulent flow and heat transfer in a channel with transverse fin arrays", *Int. J. Numerical Methods for Heat and Fluid Flow*, Vol. 10 No. 8, pp. 842-61.

Yuan, Z.X., Tao, W.Q. and Wang, Q.W. (1998), "Numerical prediction for laminar forced convection heat transfer in parallel-plate channels with streamwise-periodic rod disturbances", *Int. J. Numerical Methods in Fluids*, Vol. 28, pp. 1371-87.

Yuan, Z.X., Zhang, J.G. and Jiang, M.J. (2004), "Analytical study on coordinative optimization of convection in tubes with variable heat flux", *Science in China Ser. E*, Vol. 47 No. 6, pp. 651-8.

Zeitpun, O. and Hegazy, A.S. (2004), "Heat transfer for laminar flow in internally finned pipes with different fin heights and uniform wall temperature", *Heat and Mass Transfer*, Vol. 40 Nos 3/4, pp. 253-9.

Corresponding author
Z.X. Yuan can be contacted at: zxyuan@bjut.edu.cn